



Published in final edited form as:

J Chromatogr B Analyt Technol Biomed Life Sci. 2008 December 1; 876(1): 69–75. doi:10.1016/j.jchromb.2008.10.022.

STUDIES OF VERAPAMIL BINDING TO HUMAN SERUM ALBUMIN BY HIGH-PERFORMANCE AFFINITY CHROMATOGRAPHY

Rangan Mallik, Michelle J. Yoo, Sike Chen, and David S. Hage*

Department of Chemistry, University of Nebraska, 704 Hamilton Hall, Lincoln, NE 68588-0304, USA

Abstract

The binding of verapamil to the protein human serum albumin (HSA) was examined by using high-performance affinity chromatography. Many previous reports have investigated the binding of verapamil with HSA, but the exact strength and nature of this interaction (e.g., the number and location of binding sites) is still unclear. In this study, frontal analysis indicated that at least one major binding site was present for *R*- and *S*-verapamil on HSA, with estimated association equilibrium constants on the order of 10^4 M^{-1} and a 1.4-fold difference in these values for the verapamil enantiomers at pH 7.4 and 37°C. The presence of a second, weaker group of binding sites on HSA was also suggested by these results. Competitive binding studies using zonal elution were carried out between verapamil and various probe compounds that have known interactions with several major and minor sites on HSA. *R/S*-Verapamil was found to have direct competition with *S*-warfarin, indicating that verapamil was binding to Sudlow site I (i.e., the warfarin-azapropazone site of HSA). The average association equilibrium constant for *R*- and *S*-verapamil at this site was $1.4 (\pm 0.1) \times 10^4 \text{ M}^{-1}$. Verapamil did not have any notable binding to Sudlow site II of HSA but did appear to have some weak allosteric interactions with L-tryptophan, a probe for this site. An allosteric interaction between verapamil and tamoxifen (a probe for the tamoxifen site) was also noted, which was consistent with the binding of verapamil at Sudlow site I. No interaction was seen between verapamil and digitoxin, a probe for the digitoxin site of HSA. These results gave good agreement with previous observations made in the literature and help provide a more detailed description of how verapamil is transported in blood and of how it may interact with other drugs in the body.

Keywords

verapamil; human serum albumin; drug-protein binding; high-performance affinity chromatography

1. Introduction

The study of drug-protein binding in blood is important in determining drug transportation, distribution, metabolism and excretion [1–11]. This binding can take place with a variety of agents in blood, including proteins such as human serum albumin (HSA). HSA has a molar mass of 66.5 kDa and is the most abundant protein in serum (typical concentration, 30–50 g/L). This protein has been widely-studied in terms of its interactions with drugs and other small solutes (e.g., warfarin, digitoxin, tamoxifen and L-tryptophan), many of which interact at relatively well-defined regions on this protein [1,8–11]. These binding regions include two

*Author for correspondence: Phone, 402-472-2744; FAX, 402-472-9402; Email, dhage@unlserve.unl.edu.

Publisher's Disclaimer: This is a PDF file of an unedited manuscript that has been accepted for publication. As a service to our customers we are providing this early version of the manuscript. The manuscript will undergo copyediting, typesetting, and review of the resulting proof before it is published in its final citable form. Please note that during the production process errors may be discovered which could affect the content, and all legal disclaimers that apply to the journal pertain.

major sites (i.e., the warfarin-azapropazone site or Sudlow site I, and the indole-benzodiazepine site or Sudlow site II) [9,10], as well as some minor sites (i.e., the tamoxifen and digitoxin sites) [10,11].

One drug that binds to HSA is verapamil (see Figure 1) [12–14]. Verapamil is used to treat hypertension, angina and arrhythmia. The main mechanism of this drug is related to its inhibition of the transmembrane influx of calcium in the cells of cardiac muscle, coronary arteries and the intra-cardiac conduction system [15]. The typical therapeutic range for verapamil in human serum is 50–100 ng/mL [16], with approximately 90% of verapamil in blood being bound to proteins such as HSA (note: binding of verapamil to lipoproteins has also been reported) [17]. Verapamil has one chiral center and two enantiomeric forms: *R*-verapamil and *S*-verapamil. These enantiomers are known to bind to HSA with different strengths and *S*-verapamil has been reported to have a higher pharmacological activity than *R*-verapamil [18].

Many previous studies have examined the binding of verapamil with HSA [19–29], but the exact strength and nature of this interaction is still unclear. Table 1 summarizes the association equilibrium constants that have been reported for this system. In these past studies, HSA has been noted to have different binding strengths and stereoselectivity for the two enantiomers of verapamil [19,21,23,25,26]. The average reported association equilibrium constants for HSA with *R*- and *S*-verapamil have ranged from $1.1\text{--}1.8 \times 10^3 \text{ M}^{-1}$ at 25°C [22,24,28] up to $1.16 \times 10^5 \text{ M}^{-1}$ at 37°C [29]. However, in other studies it has been estimated that the individual *R*- and *S*-enantiomers of verapamil have association equilibrium constants of $2.6\text{--}2.7 \times 10^3$ and $0.85 \times 10^3 \text{ M}^{-1}$, respectively, at pH 7.4 and 25°C [19,23]. This large range of values indicates that there is still a significant amount of uncertainty regarding the true strength of binding between verapamil and HSA. Another unresolved factor concerns the number and types of sites that are involved in this interaction. Although previous data for this system has often been examined by using a one-site model, there is some evidence that multiple binding regions may be involved in these interactions [22,24,27,29].

The variety of binding constants that have reported for the verapamil/HSA system and the uncertainty regarding the number of binding sites for this interaction suggest that further characterization of this system is still needed. In this study high-performance affinity chromatography (HPAC) will be used to more closely examine the binding of verapamil and its enantiomers to HSA. HPAC is liquid chromatographic technique that utilizes a specific binding agent such as HSA as an immobilized ligand for the purification or analysis of sample components [1,2,30–34]. One advantage of using this method for binding studies is it can be used with site selective probes to independently examine the binding of drugs at Sudlow sites I or II on HSA, as well as at the tamoxifen and digitoxin sites [1–2,34]. In the past, HPAC has been successfully used to obtain a variety of information on drug interactions with HSA and has been shown to provide good correlation with solution-based methods (see review in Ref. [1] and references therein). These features will be used in this report to better characterize the binding strength and number of binding sites for *R*- and *S*-verapamil with HSA under physiological conditions (i.e., pH 7.4, and 37°C). HPAC will also be used with various chemical probes to determine which sites on HSA are involved in these interactions. These results will then be compared with those obtained in previous studies, giving a more complete description of how verapamil binds to HSA and of how this drug may compete with other solutes for this protein.

2. Experimental section

2.1. Reagents

The HSA (Cohn fraction V, essentially fatty acid free, > 96% pure), racemic verapamil (> 98%), *R*- and *S*-verapamil (> 98%), L-tryptophan (> 98%), *S*-warfarin (> 98%), periodic acid reagent (> 99%; an oxidizing agent), sodium borohydride (98%; a strong reducing agent), sodium cyanoborohydride (94%; a mild reducing agent), and 3-glycidioxypropyltrimethoxysilane (97%) were from Sigma (St. Louis, MO, USA). The acetic acid (> 99.7%; flammable) and sulfuric acid (95–98%; a corrosive, strong oxidizer, and carcinogenic agent) were from EMD chemicals (Gibbstown, NJ, USA). Nucleosil Si-300 (5 μm particle diameter, 300 \AA pore size) was obtained from Macherey Nagel (Düren, Germany). All aqueous solutions were prepared using water from a Nanopure system (Barnstead, Dubuque, IA, USA) and filtered using Osmonics 0.22 μm nylon filters from Fisher (Pittsburgh, PA, USA). Reagents for the bicinchoninic acid (BCA) protein assay were from Pierce (Rockford, IL, USA).

2.2. Apparatus

The HSA silica and control silica were packed into separate 2.1 mm I.D. \times 5 cm long stainless steel columns using an Alltech column slurry packer (Deerfield, IL, USA). All chromatographic studies were performed using a Jasco Pu980i pump, along with a CM4100 gradient pump and UV100 absorbance detector from Thermoseparations (Riviera Beach, FL, USA). Samples were injected using a Rheodyne LabPro valve (Cotati, CA, USA) equipped with a 20 μL sample loop. Chromatographic data were collected and processed using in-house programs written in LabView 5.1 (National Instruments, Austin, TX, USA).

2.3. Methods

The conditions used for the immobilization of HSA to silica by the Schiff base method were adapted from the literature [31,39], with all reactions being carried out at room temperature unless otherwise indicated. The control support for this material was prepared following the same procedure as described above but with no HSA being added during the immobilization reaction. Small portions of both the HSA silica and control support were washed several times with deionized water and dried under vacuum at room temperature. These dried samples were analyzed in triplicate using a BCA protein assay [40] in which HSA was the standard and the control silica was the blank. With this procedure, the final protein content of the HSA silica was found to be 28 (\pm 2) mg of HSA/g of silica (note: the value in parentheses represents a range of \pm 1 SD). The HSA silica and control support were downward slurry packed at 3500 psi (214 bar) into separate columns using pH 7.4, 0.067 M potassium phosphate buffer as the packing solution. Each column was placed into a water jacket for temperature control. When in use, these water jackets were connected to a circulating water bath and held at a temperature of 37°C for all of the chromatographic studies that were performed in this report.

All mobile phases for the chromatographic studies were degassed for at least 15 min prior to use. The elution of verapamil was monitored at 228 nm. Other injected compounds were detected at the following wavelengths: L-tryptophan, 280 nm; digitoxin, 205 nm; tamoxifen, 205 nm; *S*-warfarin, 310 nm; and sodium nitrate, 205 nm. All samples and mobile phases were prepared in pH 7.4, 0.067 M potassium phosphate buffer. In the zonal elution studies with digitoxin and tamoxifen, 2.5 mM β -cyclodextrin was also added to the pH 7.4, 0.067 M potassium phosphate buffer as a solubilizing agent [31]. Solutions containing L-tryptophan were prepared fresh daily. All other solutions were used over the course of up to two few weeks and were stored in the dark at 4°C between studies.

Frontal analysis experiments were performed using mobile phases that contained concentrations in the range of 0.5–20 μM *R*- or *S*-verapamil. These solutions were applied at a flow rate of 0.4 mL/min. This flow rate was found to be well within the range needed to establish a local equilibrium in the HSA column, in agreement with earlier results reported for other solutes [31,41] and with zonal elution studies that were performed in this current study (see following paragraph). All frontal analysis experiments were performed in at least duplicate under each set of tested conditions. The retained verapamil was eluted from the column after each study and the column was regenerated before the next application of verapamil by passing only pH 7.4, 0.067 M potassium phosphate buffer through the column. The amount of verapamil required to saturate the column was determined from the mean position of the resulting breakthrough curve [42]. The results obtained for the control column were subtracted from those for the HSA column to correct for the column void time and for secondary interactions between verapamil and the support (note: the retention factor for *R/S*-verapamil in the control column was typically 55–58% of that measured on the HSA column). A correction for the system void time was made by performing similar experiments using a 50 μM solution of sodium nitrate (i.e., a non-retained solute).

The zonal elution experiments were performed at 0.5–1.0 mL/min. A variation of less than 1% in the retention factor for each injected compound was noted as the flow rate was varied from 0.2 to 1.2 mL/min, confirming that a local equilibrium had been established as these compounds passed through the HSA column or control column under these conditions [1]. At each concentration of competing agent, triplicate injections of the analyte or desired probe compound were made. The concentrations of the injected compounds were as follows: 44 μM *S*-verapamil, 22 μM *R*-verapamil, 5 μM L-tryptophan, 20 μM *S*-warfarin, 10 μM digitoxin, or 10 μM tamoxifen. The use of these sample concentrations was sufficient to avoid any significant changes in the retention factor due to overloading effects and non-linear elution conditions (Note: variations of less than 1–2% were noted in the measured retention factors when using more dilute samples) [30,31]. The concentrations used for verapamil as a competing agent in these studies were as follows: 0–34 μM *R*-verapamil, 0–20 μM *S*-verapamil, or 0–50 μM racemic verapamil (note: the slightly different ranges used for the two verapamil enantiomers reflects the different binding strengths of these analytes to HSA and the slightly different concentrations of competing agents that were thus needed to give a particular degree of retention for these analytes). The concentrations of L-tryptophan and warfarin used as competing agents ranged from 0–50 μM and 0–6.5 μM , respectively. The mean retention time for each peak was obtained by calculating its first statistical moment [30]. The column void time was determined by injecting a 50 μM sample of sodium nitrate as a non-retained solute.

3. Results and Discussion

3.1. Frontal analysis studies

The overall binding of *S*- and *R*-verapamil with HSA was first examined by frontal analysis. In this technique a solution with a known concentration of pure analyte is continuously applied to a column that contains a fixed amount of the immobilized ligand. As the column becomes saturated, the amount of analyte eluting from the column increases and forms a characteristic breakthrough curve, as shown in Figure 2(a). The mean position of this breakthrough curve is related to the concentration of the applied analyte, the amount of active ligand in the column, and the association equilibrium constants for the binding of the analyte to the ligand. Both one-site and two-site binding models were used to fit the frontal analysis data obtained in this study, as represented by Eqns. (1) and (2), respectively, in Table 2.

Figures 2(a) and 3(a) show the results that were obtained for the application of various concentrations of *S*-verapamil to an HSA column at pH 7.4 and 37°C. Similar results were obtained for *R*-verapamil (data not shown). Plots of $1/m_{Lapp}$ versus $1/[\text{Verapamil}]$ there were

prepared for both verapamil enantiomers gave reasonably good linear behavior over the range of concentrations that were sampled in Figure 3, although a small amount of curvature was present in the plot for *S*-verapamil (note: work over a broader range of concentrations to better define this curvature was not practical in this case because of the large expense of working with the individual enantiomers of verapamil in such studies).

The graph in Figure 3(a) had a correlation coefficient of 0.995 for *S*-verapamil over the five concentrations that were sampled. The similar plot was obtained for *R*-verapamil, which gave a correlation coefficient of 0.999 ($n = 5$). Although a linear response for this type of plot would be expected for a system with 1:1 binding, as predicted by Eqn. (1), it is also possible for such a plot to have a linear region for a multi-site system if work is being performed at reasonably low analyte concentrations, as indicated by Eqn. (3) [37,43]. This second situation was of interest because a few previous studies have suggested that verapamil may have multiple binding regions on HSA with high and low affinities for this drug [22,24,27,29]. In this case, some curvature at higher applied concentrations (as noted for *S*-verapamil) would be expected according to Eqn. (2) (see detailed discussion in Ref. [37]). However, the response over the linear region at lower concentrations (or high values of $1/[\text{Verapamil}]$) can still be often used even in this situation with Eqn. (3) to obtain a preliminary estimate of the association equilibrium constant for the highest affinity site in the system [37].

The estimates for the association equilibrium constants that were obtained by using the data in Figure 3(a) with Eqn. (3) were $4.8 (\pm 1.6) \times 10^4 \text{ M}^{-1}$ for *S*-verapamil and $6.7 (\pm 1.9) \times 10^4 \text{ M}^{-1}$ for *R*-verapamil. These values fall within the general range of values of $0.85\text{--}12 \times 10^5 \text{ M}^{-1}$ that have been reported for the verapamil enantiomers or racemic verapamil at temperatures between 25°C and 37°C (see Table 1). The 1.4-fold larger association equilibrium constant that was estimated by this approach for *R*-verapamil versus *S*-verapamil at 37°C follows the same trend seen for the K_a values of these enantiomers at 25°C [21,23]. Furthermore, this difference fits with the observation that *S*-verapamil has less binding than *R*-verapamil in solutions containing HSA [23] or in serum and plasma [25,26,44].

The intercept of the linear fit produced from the plot in Figure 3(a) for *S*-verapamil, as well as the intercept for a similar plot made for *R*-verapamil, was used to examine the binding capacity for this drug on the HSA column. For a system with 1:1 binding, the inverse of this intercept should give the total moles of binding sites in the column, as predicted by Eqn. (1); however, for a multisite system the intercept is a function of both the total binding capacity and the relative amounts of high versus low affinity sites in the column, as indicated by Eqn. (3) [37]. This made the intercept of such a plot useful as a general indicator of whether multisite binding was actually present in this particular experiment.

The intercepts of the best-fit lines for plots like those in Figure 3(a) gave an apparent binding capacity of $44 (\pm 1) \text{ nmol}$ for *S*-verapamil and $43 (\pm 9) \text{ nmol}$ for *R*-verapamil on the HSA column. It was known for this column that the total amount of HSA present was $26 (\pm 2) \text{ nmol}$, as based on a measured protein content of $28 (\pm 2) \text{ mg HSA/g silica}$ and the known packing density of this support. A comparison of these numbers indicated that the binding capacity for *R*- or *S*-verapamil was at least 1.5-times higher than the total HSA protein content. It is known from previous work that the major binding sites on HSA do not have full activity when this protein is immobilized for use in an HPAC column (e.g., ~50% activity for HSA that has been immobilized by the same method as used in this current study) [31]. Thus, a binding capacity of up to 3 mol verapamil/mol soluble HSA could be expected from these results. This information indicated that this binding was occurring to at least two different types of regions on HSA for both verapamil enantiomers, as has been suggested previously [22,24,27,29]. It has also been noted earlier that a second group of sites for verapamil on HSA may involve only non-specific and/or weak binding interactions [29], which explains why these sites produce

only small amounts of curvature at high verapamil concentrations (or low $1/[\text{Verapamil}]$ values) for some of the plots in Figure 3(a) [37].

3.2. Competition between verapamil with warfarin

The goal of the next series of experiments was to determine which regions on HSA were involved in binding to verapamil. This work was conducted by using zonal elution and competition experiments. These experiments were performed by placing a known concentration of a competing agent (I) in the mobile phase while small injections of the analyte (A) were made, as illustrated in Figure 2(b). If I and A compete at a single site on ligand L and A has no other interactions with the column, Eqn. (4) in Table 2 could then be used to describe the observed retention of A [4].

The first set of zonal elution experiments examined the competition of *R/S*-verapamil with *S*-warfarin, a drug known to interact with Sudlow site I (i.e., one of the major binding sites for drugs on HSA) [2,45,46]. Initial studies using injections of racemic verapamil in the presence of *S*-warfarin gave a decrease in retention for both enantiomers as the mobile phase concentration of *S*-warfarin was increased (data not shown). Although the resolution was insufficient to separate the peaks for these two enantiomers, the fact that both shifted in the same manner indicated that the two enantiomers of verapamil had similar interactions with *S*-warfarin on HSA. The reverse study, shown in Figure 2(b), was then performed, in which *S*-warfarin was injected into the presence of racemic verapamil. This experiment gave a decrease in retention for *S*-warfarin as the concentration of verapamil was increased in the mobile phase, also indicating that *R/S*-verapamil was interacting/competing with *S*-warfarin during their binding to HSA. Identical experiments conducted on the control column demonstrated that *S*-warfarin had no appreciable amounts of non-specific binding to the support under these conditions (i.e., the retention factor on the control column for *S*-warfarin was less than 3% of that on the HSA column).

A closer analysis of the results in Figure 2(b) was performed by using Eqn. (4). The resulting plot is given in Figure 3(b). It was found that a plot of $1/(k_{S\text{-Warfarin}})$ versus $[\text{Verapamil}]$ gave a linear response with a correlation coefficient of 0.9899 ($n = 6$). According to Eqn. (4), this linear response is consistent with a model in which there is direct competition at a single type of site between *S*-warfarin and verapamil. Since *S*-warfarin is known to bind to Sudlow site I of HSA, this result suggested that verapamil was also binding to this site. This agrees with previous work in the area of CE in which racemic warfarin was found to displace and affect the binding of both *R*- and *S*-verapamil to HSA [27]; however, this past work did not determine the specific nature of this displacement (e.g., direct competition or a negative allosteric interaction). The behavior seen in Figure 3(b) not only confirms that an interaction between warfarin and verapamil can take place on HSA but indicates that this interaction is due to direct competition of warfarin and the two verapamil enantiomers at Sudlow site I.

It was possible by using Eqn. (4) and the slope and intercept of plots like those in Figure 4 to estimate the association equilibrium constant for *R/S*-verapamil at Sudlow site I. This process gave an average K_a value of $1.4 (\pm 0.1) \times 10^4 \text{ M}^{-1}$ for the verapamil enantiomers at Sudlow site I. That value was within 2 SD of the average estimated K_a of $5.8 (\pm 2.5) \times 10^4 \text{ M}^{-1}$ that was obtained when using the frontal analysis data from previous section for *R*- and *S*-verapamil and was again within the range of values reported in the literature for the high affinity site of verapamil with HSA, as shown in Table 1. This information is all consistent with a model in which Sudlow site I is the high affinity site for verapamil.

3.3 Interactions between verapamil and tamoxifen on HSA

When a binding agent such as HSA binds to two solutes (A and I) at two distinct sites, it is possible that the binding of one solute may affect the binding of other through allosteric effects. It was necessary to consider this type of effect when competition studies based on zonal elution were next performed between verapamil and tamoxifen. Tamoxifen is sometimes used as a probe for a minor binding site on HSA that is sometimes referred to as the “tamoxifen” site [1–4,11,30,35]. The interaction of verapamil with this site was examined by injecting tamoxifen as a site-selective probe while racemic verapamil was used as a mobile phase additive. Figure 4(a) shows the change in retention for tamoxifen that was observed at pH 7.4 and 37°C as the concentration of verapamil in the mobile phase was varied. Similar experiments on a control column showed that tamoxifen had no appreciable amounts of non-specific binding to the support under these conditions (i.e., less than 5% of the retention noted on the HSA column).

The plot of $1/(k_{\text{tamoxifen}})$ versus [Verapamil] that was obtained during these experiments gave a large non-linear decrease in the retention for tamoxifen (or an increase in $1/k$ for tamoxifen) as the concentration of verapamil in the mobile phase was increased from 0 to 50 μM . This behavior could be produced if there were a negative allosteric effect of verapamil on the binding of tamoxifen to HSA. This type of allosteric effect is also known to be present between warfarin (as it binds to Sudlow site I) and tamoxifen or related solutes that bind to the tamoxifen site [11,47,48].

The possible presence of an allosteric effect between the binding sites for verapamil and tamoxifen on HSA was further examined by replotting the data in Figure 4(a) according to Eqn. (5). The resulting graph is shown in Figure 4(b). This second plot gave a linear relationship with a negative slope and intercept and a correlation coefficient of 0.994 ($n = 5$). The behavior seen in this plot is what would be expected for a system in which the binding of verapamil to HSA causes a negative allosteric effect on the binding of tamoxifen to HSA. The value of the coupling constant β that was obtained from Figure 4(b) for this effect was $0.59 (\pm 0.03)$, which indicates the binding of verapamil created a decrease of 41% in the apparent binding constant for tamoxifen with HSA. This behavior is the same as seen for the effect of warfarin on tamoxifen [47,48] and further supports a model in which verapamil is binding to Sudlow site I.

3.4 Interactions between verapamil and L-tryptophan on HSA

Results from the last two sections strongly support a model in which Sudlow site I is the high affinity site for verapamil on HSA. However, further studies were conducted to see if any of the secondary interactions that were noted in the frontal analysis studies could be contributed to the interaction of verapamil with other known drug binding sites on this protein. The first of these experiments were carried out by using L-tryptophan as an injected probe. L-Tryptophan is known to bind specifically to Sudlow site II of HSA and has a well-characterized equilibrium constant for this interaction [1–4,30,35].

Figure 5(a) shows the change in retention seen for L-tryptophan at 37°C as the concentration of racemic verapamil was varied in the mobile phase. The retention of L-tryptophan on the control column was less than 8% of its retention in HSA column under these conditions, so no corrections were needed for non-specific binding for L-tryptophan in HSA column. A plot of $1/(k_{\text{L-tryptophan}})$ versus [Verapamil] made according to Eqn. (4) gave what appeared to be only small initial decrease in retention (or an increase in $1/k$), followed by random variations in the retention of L-tryptophan as the concentration of verapamil was increased further. The total size of this shift in retention was from $k = 5.9$ to 5.4 over the range of concentrations that were examined in Figure 5(a), with most of this change occurring between 0 1 μM verapamil (note:

the remainder of the retention values all overlapped within a range of ± 2 SD). The same type of behavior and a slightly larger shift of 25% in k were noted later for a newer HSA column with a higher binding capacity. Although the shift in these results was too small to effectively analyze according to Eqn. (5), these results do fit qualitatively with a model in which there is a small negative allosteric effect of verapamil on L-tryptophan but no direct competition between these two solutes as they bind to HSA.

The reverse experiment was also performed, in which L-tryptophan was used as a mobile phase additive and a small amount of verapamil was injected onto the column. The result of this study is shown in Figure 5(b). In this case a small increase in the retention of verapamil may have been produced as more L-tryptophan was placed into the mobile phase. This shift was also too small to be analyzed through the use of Eqn. (5) but is consistent with the presence of a small allosteric effect between these two solutes.

3.5 Interactions between verapamil and digitoxin on HSA

Digitoxin is sometimes used as a probe for a minor binding region on HSA that is called the "digitoxin site" [1–4,11,30,35]. The interaction of verapamil with this site was examined by injecting digitoxin as the injected probe and verapamil as a mobile phase additive. Digitoxin is known to not have any appreciable nonspecific binding to the control support used in this study [2], as confirmed by the fact that the retention of digitoxin on the control column was less than 3% of the retention for digitoxin on the HSA column.

It was found during competitive zonal elution studies that the retention measured for digitoxin changed only from 36.3 to 38.3 as the concentration of racemic verapamil in the mobile phase was increased from 0 to 50 μM (data not shown). This represented a maximum change of only 5.5% in k and was approximately same order in size as the precision for the retention factors measured in this particular study. These results indicated that there was no significant interaction between digitoxin and verapamil as they both were under bound to HSA.

CONCLUSIONS

It was found through frontal analysis indicated that at least one major binding site was present for *R*- and *S*-verapamil on this HSA. The same experiments gave overall association equilibrium constants on the order of 10^4 M^{-1} and that differed by 1.4-fold for the two verapamil enantiomers at pH 7.4 and 37°C. The presence of a second, weaker group of binding regions for verapamil was also suggested, in agreement with previous results reported in Ref. [29]. Competitive binding studies indicated that the high affinity site for verapamil on HSA was Sudlow site I (i.e., the warfarin-azapropazone site of HSA), giving an average association equilibrium constant for *R*- and *S*-verapamil of $1.4 (\pm 0.1) \times 10^4 \text{ M}^{-1}$ at this site. The identification of this binding region for verapamil fits with data obtained in previous displacement studies conducted in Ref. [27] and was confirmed in this current report by an observed allosteric interaction between verapamil and tamoxifen, as is known to occur between tamoxifen and warfarin (a probe for Sudlow site I) [47,48].

Verapamil did not bind directly to Sudlow site II but it did appear to have some weak allosteric interactions with L-tryptophan, a probe for this site. In addition, no interactions were seen between verapamil and digitoxin, a probe for the digitoxin site of HSA. The lack of direct binding of verapamil to any of the tested sites besides Sudlow site I, along with binding capacity measured in this work by frontal analysis, fit a model in which the secondary binding regions of this drug on HSA are non-specific in nature, as is also supported by data from Ref. [29]. These results, along with new information obtained in this study concerning the location and binding strength of the high affinity site for verapamil on HSA, provide an improved model

for describing the transport of verapamil in blood and in characterizing its possible interactions with other drugs in the body.

Acknowledgements

This research was supported by the National Institutes of Health under grant R01 GM044931 and was conducted in facilities that were renovated under NIH grant RR015468-01.

References

1. Hage DS. *J Chromatogr B* 2002;768:3.
2. Hage DS, Austin J. *J Chromatogr B* 2000;739:39.
3. Hage DS, Noctor TAG, Wainer IW. *J Chromatogr A* 1995;693:23. [PubMed: 7697161]
4. Hage, DS. Kirk-Othmer Encyclopedia of Chemical Technology. 5. 2004. p. 390
5. Mallik R, Wa C, Hage DS. *Anal Chem* 2007;79:1411. [PubMed: 17297940]
6. Wan H, Bergstroem F. *J Liq Chromatogr* 2007;30:681.
7. Trainor GL. *Expert Opin Drug Discovery* 2007;2:51.
8. Peters, T. All About Albumin: Biochemistry, Genetics, and Medical Applications. Academic Press; San Diego: 1995.
9. Kragh-Hansen U. *Pharmacol Rev* 1981;33:17. [PubMed: 7027277]
10. Kragh-Hansen U, Chuang VTG, Otagiri M. *Biol Pharmaceut Bull* 2002;25:695.
11. Sengupta A, Hage DS. *Anal Chem* 1999;71:3821. [PubMed: 10489529]
12. Sica DA, Prisant LM. *J Clin Hypertens* 2007;9:1.
13. Rehman SU, Basile J. *Aging Health* 2005;1:419.
14. Takhashi N, Saikawa T. *Clin Calcium* 2005;15:1651. [PubMed: 16199910]
15. Lee KS, Tsien RW. *Nature* 1983;302:790. [PubMed: 6302512]
16. Angus JA, Brazenor RM, Le Duc MA. *Clin Exp Pharmacol Physiol Suppl* 1982;6:15. [PubMed: 6956474]
17. Mohamed NAL, Kuroda Y, Shibukawa A, Nakagawa T, El Gizawy S, Askal HF, El Kommos ME. *J Chromatogr A* 2000;875:447. [PubMed: 10839164]
18. Echizen H, Manz M, Eichelbaum M. *J Cardiovasc Pharmacol* 1988;12:543. [PubMed: 2468053]
19. Ding Y, Lin B. *Chin J Chromatogr* 1999;17:138.
20. Ding Y, Lin B. *Chin J Chromatogr* 1999;17:134.
21. Ding Y, Zhu X, Lin B. *Sci China, Ser B* 1999;42:617.
22. Ding Y, Zhu X, Lin B. *Chin J Chromatogr* 1999;17:58.
23. Ding YS, Zhu XF, Lin BC. *Electrophoresis* 1999;20:1890. [PubMed: 10445331]
24. Ding YS, Zhu XF, Lin BC. *Chromatographia* 1999;49:343.
25. Mehvar R, Reynolds J. *Drug Metab Dispos* 1996;24:1088. [PubMed: 8894509]
26. Mehvar R, Reynolds JM, Robinson MA, Longstreth JA. *Pharmaceut Res* 1994;11:1815.
27. Zhu XF, Ding YS, Lin BC, Jakob A, Koppenhoefer B. *Electrophoresis* 1999;20:1869. [PubMed: 10445329]
28. Jia Z, Ramstad T, Zhong M. *J Pharm Biomed Anal* 2002;30:405. [PubMed: 12367665]
29. Lee KJ, Park HJ, Shin YH, Lee CH. *Arch Pharm Res* 2004;27:978. [PubMed: 15473671]
30. Chen J, Hage DS, Ohnmacht C. *J Chromatogr B* 2004;809:137.
31. Kim HS, Hage DS. *J Chromatogr B* 2005;816:57.
32. Mallik R, Hage DS. *J Sep Sci* 2006;29:1686. [PubMed: 16970180]
33. Mallik R, Jiang T, Hage DS. *Anal Chem* 2004;76:7013. [PubMed: 15571354]
34. Mallik, R.; Jiang, T.; Hage, DS. 40th Midwest Regional Meeting of the American Chemical Society; Joplin, MO. October 26–29 (2005); p. LIN05
35. Chen J, Fitos I, Hage DS. *Chirality* 2005;18:24. [PubMed: 16278829]

36. Walters, RR. Analytical Affinity Chromatography. Chaiken, IM., editor. CRC Press; Boca Raton, FL: 1987.
37. Tweed SA, Loun B, Hage DS. Anal Chem 1997;69:4790. [PubMed: 9406530]
38. Chen J, Hage DS. Nature Biotechnol 2004;22:1445. [PubMed: 15502818]
39. Larsson PO. Methods Enzymol 1984;104:212. [PubMed: 6371445]
40. Smith PK, Krohn RI, Hermanson GT, Mallia AK, Gartner FH, Provenzano MD, Fujimoto EK, Goeke NM, Olson BJ, Klenk DC. Anal Biochem 1985;150:76. [PubMed: 3843705]
41. Kim, HS.; Hage, DS. Handbook of Affinity Chromatography. 2. Hage, DS., editor. CRC Press; Boca Raton: 2005. p. 35
42. Hage, DS.; Xuan, H.; Nelson, MA. Handbook of Affinity Chromatography. 2. Hage, DS., editor. CRC Press; Boca Raton: 2005. p. 80
43. Mallik R, Xuan H, Guiochon G, Hage DS. Anal Biochem 2008;376:154. [PubMed: 18294445]
44. Ohara T, Shibukawa A, Nakagawa T. Anal Chem 1995;67:3520. [PubMed: 8686900]
45. Loun B, Hage DS. Anal Chem 1994;66:3814. [PubMed: 7802261]
46. Loun B, Hage DS. Anal Chem 1996;68:1218. [PubMed: 8651495]
47. Chen J, Hage DS. Anal Chem 2006;78:2672. [PubMed: 16615779]
48. Sjöholm I, Ekman B, Kober A, Ljungstedt-Pahlman I, Seiving B, Sjödin T. Mol Pharmacol 1979;16:767. [PubMed: 530258]

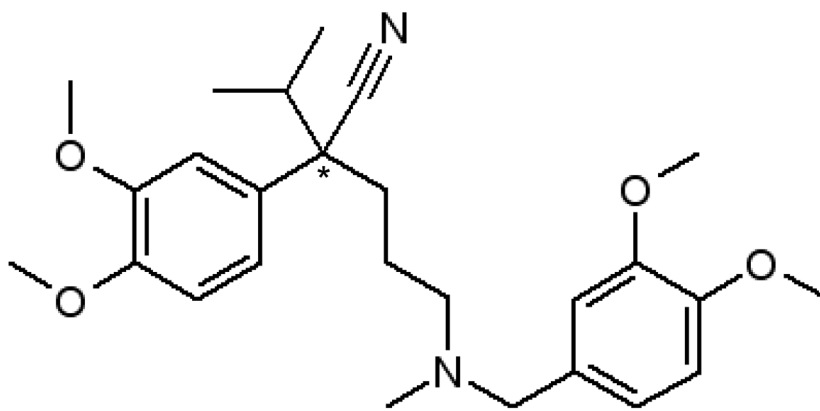


Figure 1. Structure of verapamil. The asterisk (*) shows the location of the chiral center.

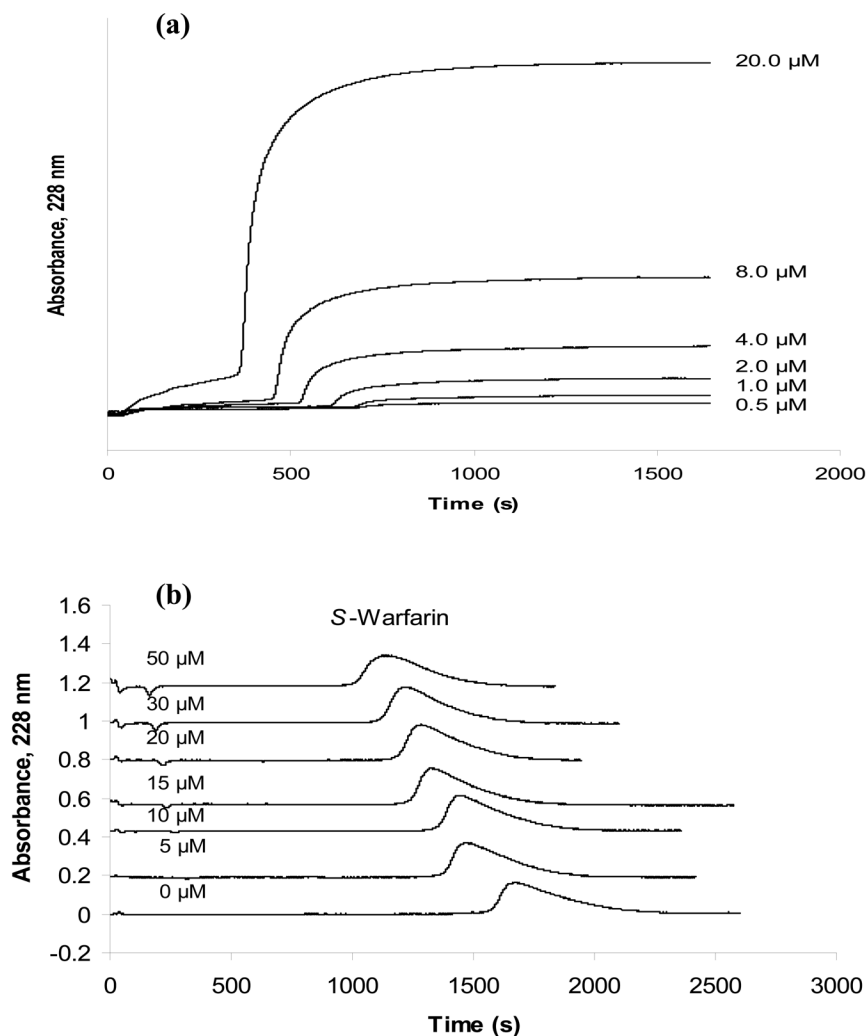


Figure 2.

Typical chromatograms obtained on an HSA column during (a) frontal analysis experiments with *S*-verapamil and (b) competitive experiments performed by zonal elution in which *S*-warfarin was the injected analyte and racemic verapamil was used as a mobile phase additive. The concentrations that are shown represent the concentration of (a) *S*-verapamil or (b) racemic verapamil that was applied in to the HSA column. These studies were conducted at 37°C in the presence of pH 7.4, 0.067 M phosphate buffer. Other experimental conditions are given in Section 3.3.

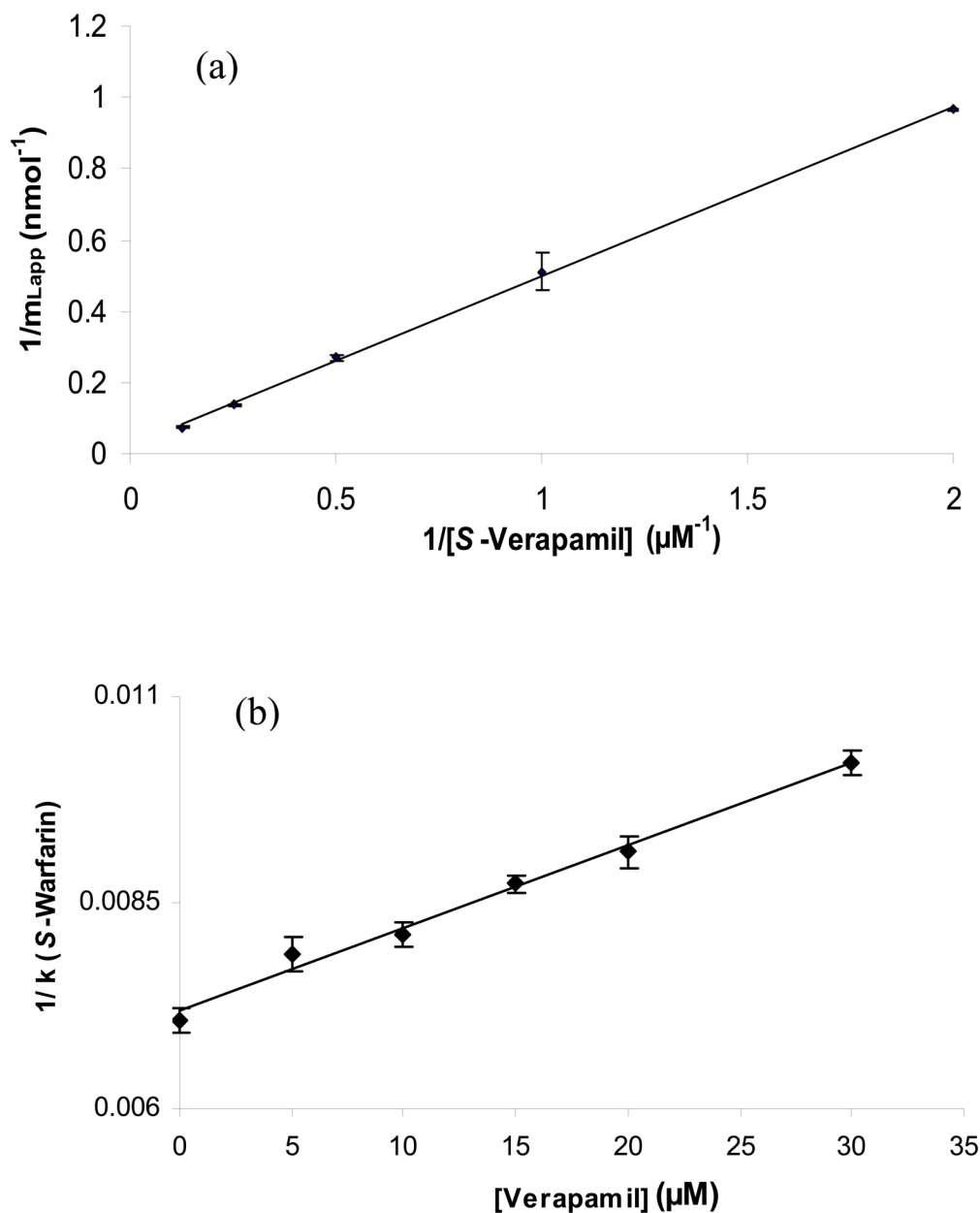


Figure 3.

Examples of (a) frontal analysis results and (b) zonal elution competition studies for verapamil on an HSA column. The plot of $1/m_{L,app}$ versus $1/[\text{Verapamil}]$ in (a) was prepared according to Eqns. (1) or (3) for *S*-verapamil, giving a best fit line of $y = 0.47 (\pm 0.01)x + 0.023 (\pm 0.001)$ with a correlation coefficient of 0.999 ($n = 5$). The plot in (b) of $1/k$ versus $[\text{Verapamil}]$ for injections of *S*-warfarin in the presence of racemic verapamil gave a best-fit line of $y = 1.0 (\pm 0.1) \times 10^{-4}x + 7.2 (\pm 0.1) \times 10^{-3}$ with a correlation coefficient of 0.989 ($n = 6$). The numbers in parentheses and the error bars represent a range of ± 1 SD. All of these studies were conducted at 37°C in the presence of pH 7.4, 0.067 M phosphate buffer. Other experimental conditions are given in Section 2.3.

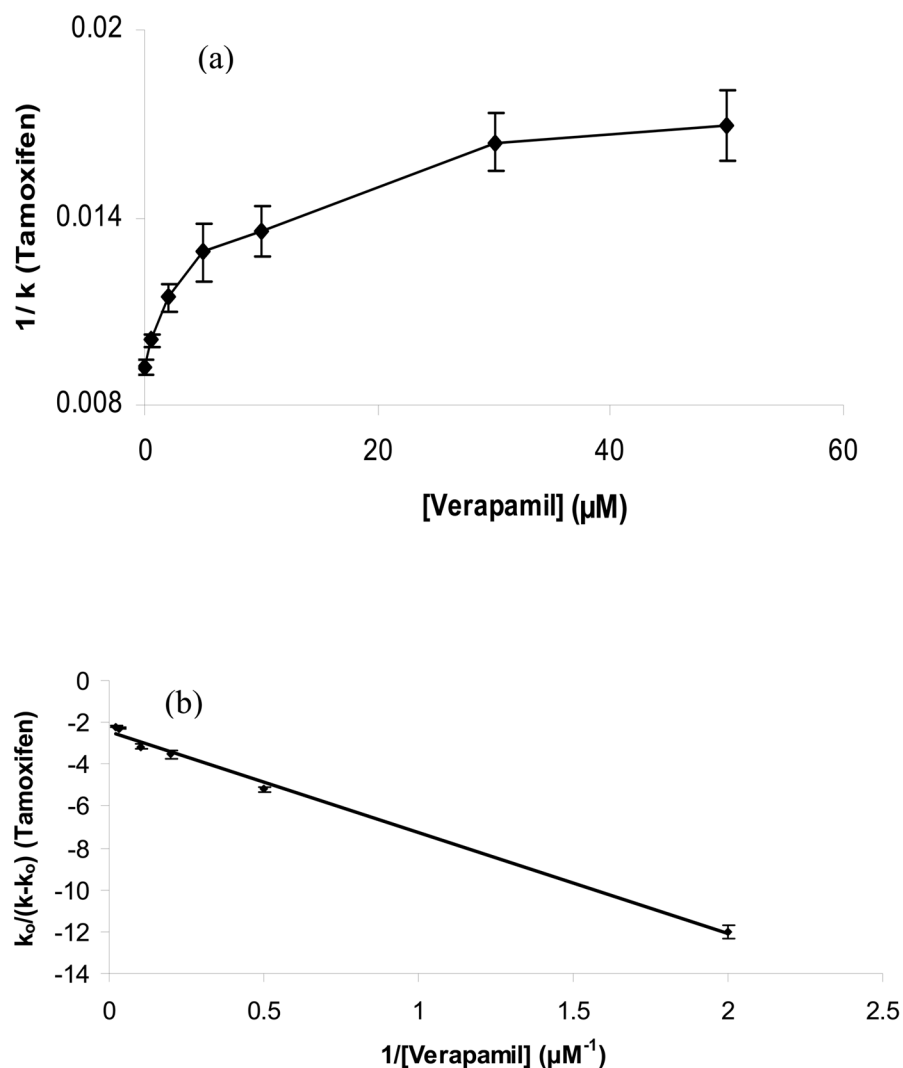


Figure 4. Zonal elution plots of (a) $1/k$ versus $[\text{Verapamil}]$ according to Eqn. (4) and (b) $k_0/(k-k_0)$ versus $1/[\text{Verapamil}]$ according to Eqn. (5) for injections of tamoxifen in the presence of mobile phases containing various concentrations of racemic verapamil. The best-fit line in (b) was $y = -4.89 (\pm 0.18)x - 2.42 (\pm 0.16)$, with a correlation coefficient of 0.998 ($n = 6$). The numbers in parentheses and the error bars represent a range of ± 1 SD. These studies were conducted at 37°C in the presence of pH 7.4, 0.067 M phosphate buffer. Other experimental conditions are given in Section 2.3.

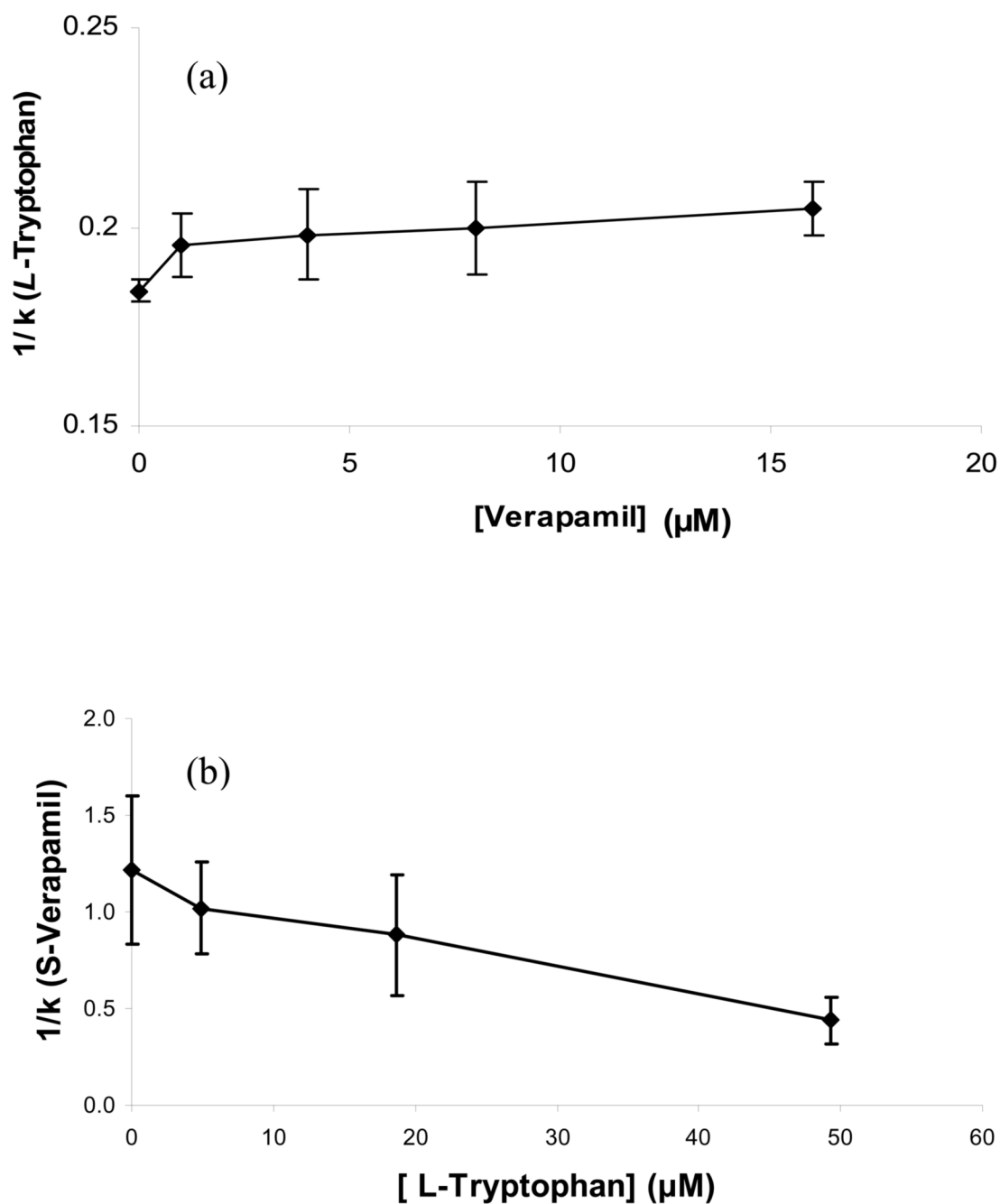


Figure 5. Competition studies performed by zonal elution for (a) the injection of L-tryptophan in the presence of racemic verapamil as a mobile phase additive or (b) the injection of S-verapamil in the presence of L-tryptophan as a mobile phase additive. The numbers in parentheses and the error bars represent a range of ± 1 SD. These studies were conducted at 37°C in the presence of pH 7.4, 0.067 M phosphate buffer. Other experimental conditions are given in Section 2.3.

Table 1
Results of previous studies examining binding of verapamil to HSA

Method (Conditions)	Association Equilibrium Constant(s) (M^{-1})	Reference
Capillary electrophoresis/frontal analysis (pH 7.4, 25°C)	R-Verapamil, $K_a = 2.67 (\pm 0.44) \times 10^3$	23 ^a
Capillary electrophoresis/liquid pre-column (pH 7.4, 25°C)	S-Verapamil, $K_a = 0.85 (\pm 0.11) \times 10^3$	21 ^a
	R-Verapamil, $K_a = 2.7 (\pm 0.44) \times 10^3$	
Capillary electrophoresis/frontal analysis (pH 7.4, 25°C)	S-Verapamil, $K_a = 0.84 (\pm 0.16) \times 10^3$	22,24 ^b
Capillary electrophoresis/frontal analysis (pH 7.4, 25°C)	Racemic verapamil, $K_a = 1.69 (\pm 0.13) \times 10^3$ to $1.79 (\pm 0.70) \times 10^3$	
Capillary electrophoresis/frontal analysis (pH 7.4, 25°C)	Racemic verapamil, $K_a = 1.10 (\pm 0.03) \times 10^3$	28
Equilibrium dialysis (pH 7.4, 37°C)	Racemic verapamil, $K_a = 1.16 \times 10^5$ and 6×10^3	29

^aThe same authors working with apparently the same system report in Ref. 19 an essentially identical value for *R*-verapamil but $K_a = 8.5 (\pm 0.1) \times 10^3 M^{-1}$ for *S*-verapamil; this appears to be the result of a typographical error.

^bThis range of values was obtained by using several data analysis methods for the same set of experimental results.

Table 2
Models and equations used to fit frontal analysis and zonal elution data

Method & Model [Reference]	Equation ^a	
<i>Frontal analysis:</i>		
One-site model [1]	$\frac{1}{m_{Lapp}} = \frac{1}{(K_a m_L [A])} + \frac{1}{m_L}$	(1)
Two-site model [37]	$\frac{1}{m_{Lapp}} = \frac{1 + K_{a1}[A] + \beta_2 K_{a1}[A] + \beta_2 K_{a1}^2[A]^2}{m_L \{(\alpha_1 + \beta_2 - \alpha_1 \beta_2) K_{a1}[A] + \beta_2 K_{a1}^2[A]^2\}}$	(2)
	$\lim_{[A] \rightarrow 0} \frac{1}{m_{Lapp}} = \frac{1}{m_L \{(\alpha_1 + \beta_2 - \alpha_1 \beta_2) K_{a1}[A] + \frac{(\alpha_1 + \beta_2^2 - \alpha_1 \beta_2^2)}{m_L (\alpha_1 + \beta_2 - \alpha_1 \beta_2)^2}\}}$	(3)
<i>Zonal elution:</i>		
One-site direct competition [4]	$\frac{1}{k} = \frac{K_I V_M [I]}{K_a m_L} + \frac{V_M}{K_a m_L}$	(4)
Two-site allosteric effect [38]	$\frac{k_0}{(k_0 - k)} = \left[\frac{1}{(\beta_{I \rightarrow A} - 1)} \right] \left[1 + \left(\frac{1}{K_{IL} [I]} \right) \right]$	(5)

^aSymbols: m_{Lapp} , moles of applied analyte at the mean point of a breakthrough curve; $[A]$, concentration of applied analyte; m_L , total moles of binding sites that bind to A in Eqns. (1)–(3), or moles of sites at which I and A compete in Eqn. (4); K_{aI} , association equilibrium constant for the highest affinity site for A in a multi-site system; α_1 , fraction of all binding sites that belong to the high affinity sites for A; β_2 , ratio of the association equilibrium constants for the low versus high affinity sites in a two-site system; V_M , void volume; $[I]$, concentration of competing agent; K_a is the association equilibrium constant for the binding of A to a ligand; K_I , association equilibrium constant for I at its site of competition with A; k , retention factor for A; k_0 , retention factor for A in the absence of I.